Performance Analysis of Solar Desalination Systems

T. V. Arjunan, H. S. Aybar, Jamel Orfi and S. Vijayan

Abstract Rapidly growing population of the world increases the demand for clean and freshwater. Solar desalination is a simple and environment-friendly process adopted for the conversion of saline and brackish water into potable drinking water. The solar desalination process mainly depends on the system design, operational and climatic conditions and is improved by many methods such as incorporating energy storage material, wick materials, and reflectors. The simple and widely accepted solar desalination system is of solar still. The performance of solar still is highly influenced by various factors such as water depth, basin materials, transparent glass angle, water–glass temperature difference, and absorber area. Moreover, the productivity of freshwater varies according to system design features and technical competence of the system. The purpose of this chapter is to explore the basic theoretical method used for the evaluation of a simple solar desalination system performance. This chapter also presents a case study to investigate the effect of few design and operational parameters on the performance.

Keywords Performance · Solar desalination · Solar still

1 Introduction

Energy and water demands in India, Saudi Arabia, China, and other countries are becoming a concern due to their growing rates and to the strong reliance of those countries on greenhouse gas-producing fossil fuels. Solar energy is identified as one of the most promising pillars for sustainable energy and water systems. In fact, the use of solar energy particularly as concentrated solar power and photovoltaic to generate

T. V. Arjunan (✉) · S. Vijayan
Coimbatore Institute of Engineering and Technology, Coimbatore 641109, India
e-mail: arjun_nivi@yahoo.com

H. S. Aybar
Bozok University, Medrese Mahallesi Adnan Menderes, Bulvari No: 118, 66200 Yozgat, Turkey

J. Orfi
College of Engineering, King Saud University, 11421 Riyadh, Kingdom of Saudi Arabia

A. Kumar and O. Prakash (eds.), *Solar Desalination Technology*,
Green Energy and Technology, https://doi.org/10.1007/978-981-13-6887-5_4

electricity and/or produce potable water is expected to take up higher shares in the world. Solar energy has been used since a long time to produce potable water. Various combinations of solar energy and desalination systems have been designed, built, and tested. Such integrated systems can be simple and small such as solar stills where few liters of freshwater is produced daily or complex with various sub-components such as large-scale solar power desalination plants with capacities of thousands of cubic meter per day.

The classification of solar desalination systems can be based on several criteria. However, one can generally classify them based on their capacity in terms of amount of produced freshwater, i.e., small-, medium- and large-scale systems, on how the solar energy is used directly or indirectly and also on the type of the energy used. Solar still is a simple device, which converts saline water into potable water for a small-scale level and it can be developed using readily available low-cost materials. No skilled labor is required to maintain the system. In spite of many advantages, the uses of this application are very limited due to low production of freshwater.

The researchers all over the world have implemented various techniques in operation and design parameters of solar desalination system to improve the performance. The productivity can be improved by improving radiation absorption capacity in the solar still by providing different absorption materials such as charcoal pieces [1] and dye materials [2]. The materials such as charcoal, black ink, and bitumen improved the productivity by 18.42, 6.87, and 25.35%, respectively [3]. To improve the performance of the system during night hours and cloudy weather conditions, different types of energy storage mediums are placed in the basin to store the excessive energy available during peak sunshine hours [4–11]. Increasing the surface area of the basin by using wick materials [12–14] also improves the performance of the system. Solar still performance can be improved by the use of phase-change materials [15–19]. Alharahsheh et al. [20] developed a solar still incorporated with phase-change material (PCM), coupled with a solar flat plate collector, which produced 40% of the total yield after sunset. Adding nanofluid with the basin water also influences the performance of the solar still [21–26]. Sharshir et al. [27] improved the output of the still with the addition of copper oxide and graphite nanoparticles for various basin water depths. The results show that the output is improved by 53.95 and 44.91% using graphite and the copper oxide micro-flakes, respectively. Integrating vacuum pump, additional condenser, solar flat plate, solar ETC collector, solar pond, etc. with solar desalination system are performing better than the conventional system [28–32]. Rahimi-Ahar et al. [33] developed a vacuum humidification dehumidification desalination system, comprised of a humidifying unit, solar air and water heaters, a liquid vacuum pump, and a condenser. The system produced the desalinated water at the rate of 1.07 l/h m^2 with the optimum operating parameters.

The performance analysis of the solar desalination system can also be studied using the theoretical analysis by solving the energy balance equations of the elements of the system. When integrating or modifying solar desalination system with different materials or devices, the theoretical analysis for such systems may differ from the conventional one. Many researchers are developing a theoretical model for various design parameters such as inlet water temperature, single and double slope, glass

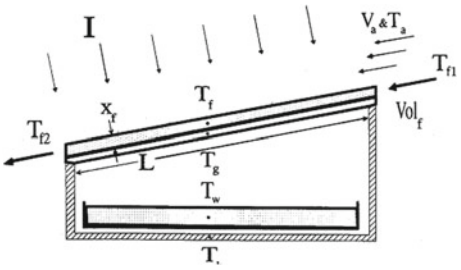

Fig. 1 Solar still with water film cooling [35]

angle, stepped basin. It is interesting to see from the literature that various theoretical models developed for different materials and devices (flat plate and ETC collector, internal external condenser) are integrated with solar stills. The analyses are also extended by the investigators for various design modifications with internal and external reflectors integrated into solar still to redirect the radiation available in and around to the basin.

It is well known that the desalinated water production of a simple solar still mainly depends on the temperature difference between the condensing surface (glass cover) and the basin water temperature. Several investigators have attempted to increase the temperature difference through various techniques such as reducing the temperature of condensing surface or/and increasing the temperature of basin water. El-Samadony and Kabeel [34] proposed a theoretical model to analyze the stepped solar still by writing energy balance for four regions: glass cover, basin, saline water, and water film cooling. The authors have pointed that for film water cooling analysis requires the inlet and exit temperatures of cooling water. The developed theoretical model has a very good agreement with their previous experimental work. Mousa [35] have numerically studied the performance of the solar still with film cooling parameters and reported that the efficiency was increased by 20% in their numerical study with the usage of water film cooling (Fig. 1).

A theoretical model was developed by Mazraeh et al. [36] for a solar still combined with PV-PCM module and the model was derived from the fundamental energy/exergy balance equations. They have also investigated the electrical and thermal performance of still for various design and operating parameters such as PV-PCM module, number of ETC, and water depth. They found that theoretical results were almost close to their experimental results. Dumbka and Mishra [37] carried out a numerical study of a still, which is suitable for coastal areas with different models such as Clark, Dunkle, Tsilingiris, Kumar and Tiwari, and modified Spalding's mass transfer theory. Muftah et al. [38] developed a theoretical model to predict the performance of the stepped solar still (Fig. 2) before and after modification. They derived the model from the fundamental energy balance equations written for each of the still elements such as glass cover, basin water, and absorber plate. The results revealed the considerable variation in the mean values of each evaluation parameters. Also, they highlighted that the modified stepped solar still yields 29% higher yield than the simple stepped solar still.

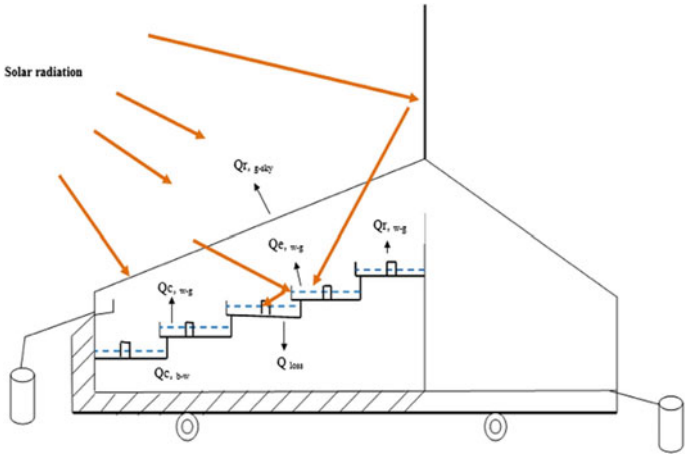

Fig. 2 Stepped solar still [38]

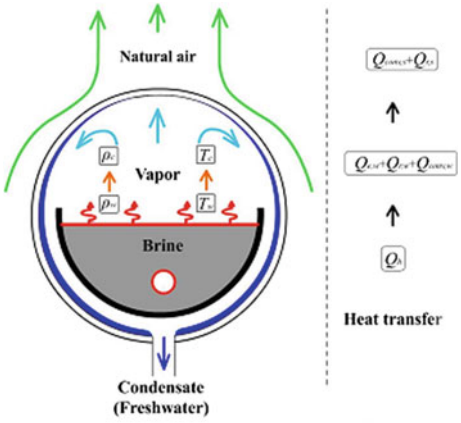

Fig. 3 Schematic of heat and mass transfer process in a single effect TSS [39]

Xie et al. [39] developed a new type of dynamic model to predict the performance of the tubular solar still (TSS) (Fig. 3) working under vacuum condition. The result shows that the new system was more efficient than the still works under normal operating conditions.

Naroei et al. [40] designed and developed stepped solar still coupled with a PVT (photovoltaic thermal water collector and also they derived a transient thermal model. The numerical results indicated the average error percentage in the range of 5.76–6.66% for the temperature values of the elements. They have also reported that the PVT collector has enhanced the freshwater production by 20% and the energy efficiency by more than 2 times (Fig. 4).

Rahbar et al. [41] performed computational simulation on triangular and tubular solar stills (Fig. 5) to analyze the flow behavior of air inside the enclosures. They

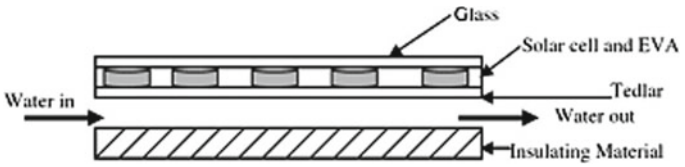

Fig. 4 PVT collector [40]

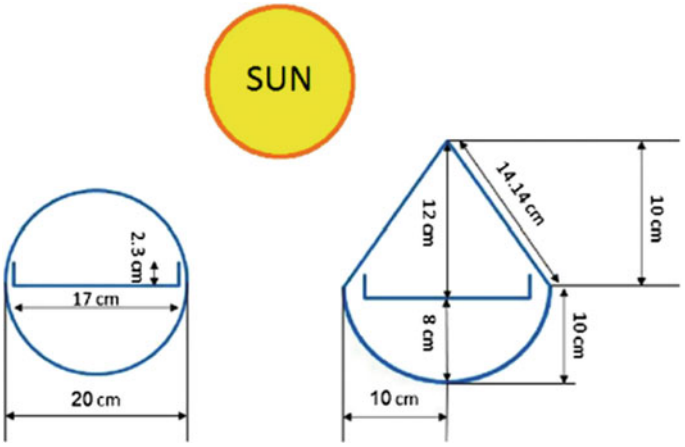

Fig. 5 Cross-sectional view of tubular and triangular stills [41]

found that that there is a formation of recirculation zone in both solar stills and which influences the output of the stills. The freshwater production in tubular solar still was higher than the triangular still about 20% due to the reason of greater strength of the recirculation zone in tubular still. The fabrication cost of the triangular still was lower than the tubular solar still which leads to low water purification cost.

A theoretical model was formulated by Kalbasi et al. [42] for the solar still with single and double effect. The theoretical results were validated through the experimental study. The distilled water production depends on the basin water temperature as well as the temperature difference between the condensing surface and the basin water. They concluded that the production of the solar still enhanced about 94% when compared with the conventional still by separating the condensing surface from the solar radiation falling surface (Fig. 6).

A new type of modified solar still was developed by Malaeb et al. [43] with a rotating drum to enhance the productivity of the system. A black painted rotating hollow drum was fabricated with the light-weight material to facilitate the rotation. In order to evaluate the performance of the system, the theoretical model was developed with different mathematical correlations to estimate the heat transfer coefficients and further the model was calibrated and validated with the experimental observations. The calibrated model was used to analyze the effect of the significant operating

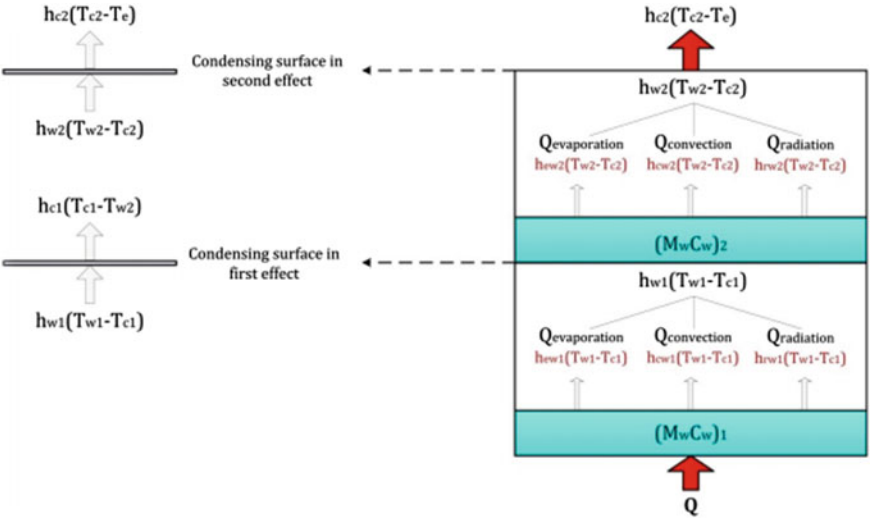

Fig. 6 Energy balance of double effects solar still Kalbasi et al. [42]

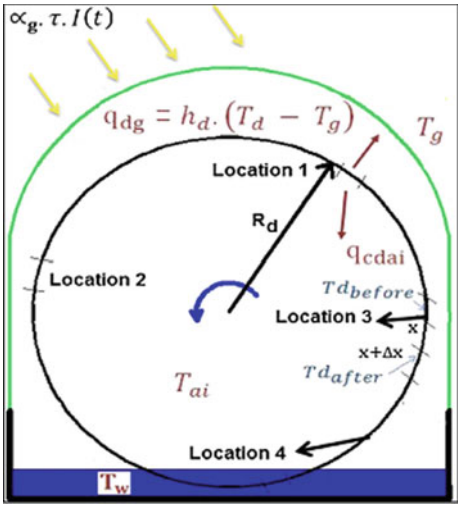

Fig. 7 Energy diagram for modified solar still with rotating drum [43]

parameters such as saline water depth, speed of rotating drum, wind speed, solar insolation, and temperature of the elements (Fig. 7).

It is understood from the literature survey that numerous research work are going on simple-, medium-, and large-scale solar desalination system all over the world for improving its performance. The thermal performance of solar desalination systems is influenced by various operational and design parameters such as water depth, temperature of inlet water, tilt angle and thickness of glass, additional condensers, reflectors, phase-change materials, flat plate and ETC collectors, and nanofluids. To

develop or understand a small- or large-scale solar desalination system, it is very much essential to learn the basic concept and theory behind the system. In order to meet this requirement, the proposed chapter deals about theoretical approach to predict the performance of a simple solar desalination system. The same procedure may be followed to the medium and large-scale solar desalination system with consideration of all parameters. The objective of this chapter is to discuss the theoretical approach which has been used to assess the thermal performance of simple solar desalination system. This chapter also presents the performance analysis of simple solar still along with a case study with various influencing parameters.

2 Theoretical Modeling of Simple Solar Desalination System

Numerous research findings were reported on superior design for solar desalination devices through the experimental study methods. In general, the experimental investigations with solar desalination systems are pricey, protracted, and prolonged. Developing a mathematical model for solar desalination systems is an attractive alternative solution to develop and investigate enhanced designs under different operational and climatically conditions. It can be established by energy balance equations for each element in the system. The theoretical model helps the researcher to design for a required capacity with minimum time and cost. Presently available advanced computing tools also make the theoretical analysis more accurate with least time and faster rate. The accuracy of the mathematical model is highly depending on its energy balance equations formulation of the system.

The performance of the still can be predicted with the use of energy balance equations written based on the heat and mass transfer operation. The following section presents the development of the theoretical model for describing the transient behavior of the still. The energy balance equations are written for all the functional elements of the simple still, such as glass cover, basin liner provided on the sidewalls, water in the basin. Figure 8 shows the various heat transfer quantities and temperature elements involved in the operation of the still.

The energy balance equations for the simple still shown in Fig. 8 have been written with the following assumptions [44]

- Basin water depth is constant.
- Film condensation occurs at the glass cover.
- The heat capacities of the material are negligible.
- The still is completely sealed (i.e., No leak).
- The temperature gradient across the thickness of glass cover and water depth is negligible.
- Still works under quasi-steady-state condition.

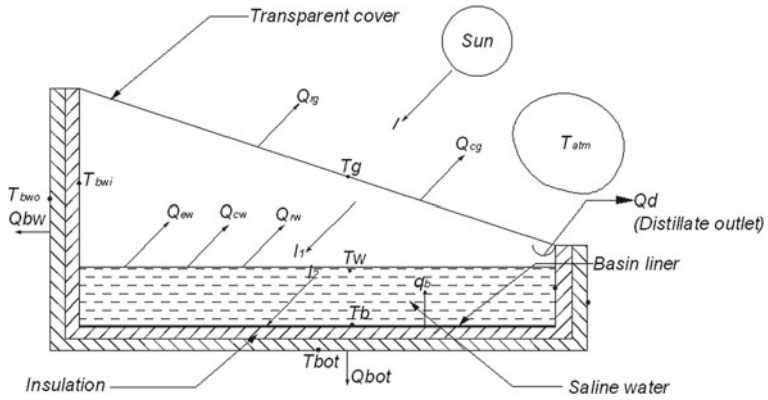

Fig. 8 Energy components of conventional solar still [44]

2.1 Energy Balance for the Water Mass in the Still

The energy balance equation for the water mass present in the still basin is written as follows by referring Fig. 8

$$I_1 + Q_b + C_w \frac{dT_w}{dt} = Q_{cw} + Q_{rw} + Q_{ew} + I_2 \tag{1}$$

where Q_b—convective heat transfer from basin to water, C_w—heat capacity of water in the basin, T_w—basin water temperature, Q_{ew}—evaporative heat transfer from water to glass, Q_{rw}—radiative heat transfer from water to glass, Q_{cw}—convective heat transfer from water to glass, I_1—solar irradiation received by the water in the still after passing through the glass cover, and I_2—solar irradiation falling on the basin liner after passing through glass and water in the still, can be determined as follows:

$$I_1 = (1 - \alpha_g)I \tag{2}$$

$$I_2 = (1 - \alpha_g)(1 - \alpha_w)I \tag{3}$$

where I is the global solar radiation in W/m^2, α_g is the radiation absorptivity of glass cover, and α_w is the radiation absorptivity of the water.

The heat transfer from the water surface in the basin to the glass cover of the still occurs in two modes, i.e., convection and radiation. The convective heat transfer from the water surface to glass cover is happening through the humid air, which can be expressed as

$$Q_{cw} = h_{cw} A_w (T_w - T_g) \tag{4}$$

where h_{cw} is the convective heat transfer coefficient of water surface to the glass cover, A_w is the cross-sectional area of the water basin, and T_g is the glass cover temperature. The difference in temperature of water in basin and the glass cover results in radiation heat transfer, which can be estimated using the Stefan–Boltzman's law as mentioned below:

$$Q_{rw} = h_{rw} A_w (T_w - T_g) = \varepsilon_{eff} A_w \sigma (T_w^4 - T_g^4) \tag{5}$$

$$h_{rw} = \varepsilon_{eff} \sigma ((T_w^2 + T_g^2)(T_w + T_g)) \tag{6}$$

where h_{rw} is the radiative heat transfer coefficient from water to glass cover, σ, Stefan-Boltzman's constant, 5.67×10^{-8} K^{-4}, ε_{eff} is the effective emittance of water surface to the glass cover.

Apart from the above, a portion of heat is utilized for evaporating the water from the basin (Q_{ew}), which can be given as

$$Q_{ew} = h_{ew} A_w (T_w - T_g) \tag{7}$$

2.2 Energy Balance for the Glass Cover

The energy balance equation for the glass cover of the still can be written as

$$Q_{rg} + Q_{cg} + I_1 = I + Q_{ew} + Q_{rw} + Q_{cw} \tag{8}$$

where I is the solar irradiation falling on the glass cover of the still, Q_{rg} is the radiative heat transfer from glass cover to atmosphere, and Q_{cg} is the convective heat transfer from glass cover to atmosphere.

$$Q_{rg} = \varepsilon_g A_g \sigma (T_g^4 - T_s^4) = h_{rg} A_g (T_g - T_a) \tag{9}$$

where A_g is the aperture area of glass cover, h_{rg} is the radiation heat transfer coefficient between glass and atmosphere, T_a denotes the atmosphere temperature, and T_s is the sky temperature and is taken as 6 °C less than ambient temperature [45].

The convective heat transfer from glass cover of the still to the atmosphere can be determined using the following expression

$$Q_{cg} = h_{cg} A_g (T_g - T_a) \tag{10}$$

where h_{cg} is the convective heat transfer coefficient between glass and atmosphere.

2.3 Energy Balance for the Basin Liner

The basin liner is the material, glued on to the basin area to improve the productivity of the still and the energy balance equation for the basin liner of the still can be written as

$$I = Q_{\mathrm{b}} + Q_{\mathrm{bot}} \tag{11}$$

The heat from the liner is transferred to the water and a small quantity of heat lost to the atmosphere through the bottom side of the basin. The quantity of heat transferred to the water from the basin liner (Q_{b}) is expressed as

$$Q_{\mathrm{b}} = h_{\mathrm{b}} A_{\mathrm{b}} (T_{\mathrm{b}} - T_{\mathrm{w}}) \tag{12}$$

where h_{b} is the convective heat transfer coefficient between basin liner and water.

The heat loss to the atmosphere (Q_{bot}) from the basin can be determined using the following equation

$$Q_{\mathrm{bot}} = U_{\mathrm{bot}} A_{\mathrm{b}} (T_{\mathrm{b}} - T_{\mathrm{a}}) \tag{13}$$

where U_{bot} denotes the overall heat transfer coefficient between water basin liner to atmosphere.

In order to determine the temperature values of the components, Eqs. (2)–(4), (6), and (7) are substituted in Eq. (1)

$$\frac{\mathrm{d}T_{\mathrm{w}}}{\mathrm{d}t} + T_{\mathrm{w}} \left(\frac{h_{\mathrm{tw}} + h_{\mathrm{b}}}{C_{\mathrm{w}}} \right) = \frac{1}{C_{\mathrm{w}}} \left(\alpha_{\mathrm{w}} I (1 - \alpha_{\mathrm{g}}) + h_{\mathrm{tw}} T_{\mathrm{g}} + h_{\mathrm{b}} T_{\mathrm{b}} \right) \tag{14}$$

It is similar to the differential equation format of $\frac{\mathrm{d}T_{\mathrm{w}}}{\mathrm{d}t} + a_1 T_{\mathrm{w}} = f_1$; then, the solution of Eq. (14) is

$$T_{\mathrm{w}} = \frac{f_1}{a_1} \left(1 - \mathrm{e}^{-a_1 t} \right) + T_{\mathrm{wi}} \mathrm{e}^{-a_1 t} \tag{15}$$

where

$$a_1 = \left(\frac{h_{\mathrm{tw}} + h_{\mathrm{b}}}{C_{\mathrm{w}}} \right) \tag{16}$$

$$f_1 = \frac{1}{C_{\mathrm{w}}} \left(\alpha_{\mathrm{w}} I \left(1 - \alpha_{\mathrm{g}} \right) + h_{\mathrm{tw}} T_{\mathrm{g}} + h_{\mathrm{b}} T_{\mathrm{b}} \right) \tag{17}$$

where $h_{\mathrm{tw}} = h_{\mathrm{rw}} + h_{\mathrm{cw}} + h_{\mathrm{rw}}$.

In order to solve Eq. (15), certain assumptions have been made, which are listed below:

(i) Initial water temperature $T_{\text{wat } t=0} = T_{\text{wi;}}$
(ii) The coefficient a_1 is constant.

Rearranging Eq. (8) by substituting (9), (10), (2)–(6), and (7)

$$\overline{T_{\text{g}}} = \frac{\alpha_{\text{g}} I_1 + h_{\text{tw}} T_{\text{w}} + h_{\text{tg}} \overline{T_{\text{a}}}}{h_{\text{tw}} + h_{\text{tg}}} \tag{18}$$

where $h_{\text{tg}} = h_{\text{cg}} + h_{\text{rg}}$.

Rearranging Eq. (11) by substituting (12) and (13),

$$\overline{T_{\text{b}}} = \frac{\alpha_{\text{b}} I_2 + h_{\text{b}} T_{\text{w}} + U_{\text{bot}} \overline{T_{\text{a}}}}{h_{\text{tw}} + U_{\text{bot}}} \tag{19}$$

The theoretical values of the system can be determined by adopting suitable numerical simulation methods and the initial temperature values of the still elements are assumed to be equal to ambient temperature. Various internal and external heat transfer coefficients can be estimated from the known initial temperatures. Using these values along with climatic parameters, T_{g}, T_{w}, and T_{b} are calculated from Eqs. (15), (18), and (19), respectively, for required time intervals. After determining the new temperature values of glass cover, water and basin, the procedure is repeated with the new values of T_{g}, T_{w}, and T_{b} for additional time intervals. After finding out the values of T_{w} and T_{g}, the theoretical hourly yield can be evaluated from equation.

$$m_{\text{w}} = \frac{A_{\text{w}} Q_{\text{ew}} 3600}{h_{\text{fg}}} \tag{20}$$

2.4 External Heat Transfer

The heat transfer in a solar desalination system is classified as internal and external heat transfer depending on energy transfer in or out the solar still [46–50]. The internal heat transfer is responsible for converting saline or brackish water into freshwater and the transport it in vapor form leaving impurities behind in the basin itself, while the external heat transfer occurs across the surrounded space and is responsible for the condensing pure vapor as pure water. Also the external heat transfer describes the clear picture of the energy balance of the system. The discussions about the internal heat transfer have been given in the previous section, and the external heat transfer is discussed in this section.

In solar distillation system, the energy transfer that occurs within the system or between the system and surrounding are by any one of the basic modes of heat transfer like conduction, convection, and radiation or combinations. It is necessary to study the energy flow between the system and surrounding to analyze the performance of the solar distillation system. The detailed step-by-step procedure to analyze the external heat transfer is given in this section.

The energy balance equations for the complete still shown in Fig. 8 is written as follows:

$$I = Q_{\mathrm{d}} + Q_{\mathrm{rg}} + Q_{\mathrm{cg}} + Q_{\mathrm{bw}} + Q_{\mathrm{sw}} + Q_{\mathrm{bot}} + Q_{\mathrm{sww}} \tag{21}$$

where I is the available solar energy and the energy is being transferred to the other components of the system. For the production of distilled water, a portion of energy is used, which can be estimated using the following equation

$$Q_{\mathrm{d}} = m_{\mathrm{w}} h_{\mathrm{fg}} \tag{22}$$

where m_{w} is the quantity of water produced in kg and h_{fg} is the latent heat of water. A small quantity of heat loss occurs from the glass cover to the atmosphere through radiation and also convection. The radiative and convective heat loss can be estimated from the following equations,

$$\text{Radiation heat loss} \quad Q_{\mathrm{rg}} = \varepsilon_{\mathrm{g}} \sigma A_{\mathrm{g}} \left(T_{\mathrm{g}}^4 - T_{\mathrm{sky}}^4 \right) \tag{23}$$

$$\text{Convection heat loss} \quad Q_{\mathrm{cg}} = h_{\mathrm{cg}} A_{\mathrm{g}} \left(T_{\mathrm{g}} - T_{\mathrm{a}} \right) \tag{24}$$

where ε_{g} is the emissivity of the glass, σ denotes Stefan–Boltzmann constant (5.67×10^{-8}, $\mathrm{W/K^4}$), A_{g} denotes surface area of the glass in $\mathrm{m^2}$, T_{g}, T_{sky}, and T_{a} are the temperatures of glass cover, sky, and ambient, respectively, and h_{cg} is the convective heat transfer coefficient in $\mathrm{W/m^2\ K}$.

The amount of heat lost from the back and front walls of the still through conduction can be determined from Eq. (25),

$$Q_{\mathrm{bw}} = \frac{T_{\mathrm{bwi}} - T_{\mathrm{bwo}}}{R_{\mathrm{bw}}} \tag{25}$$

The conductive heat resistance of the back wall surface is given as

$$R_{\mathrm{bw}} = \frac{1}{A_{\mathrm{bw}}} \left[\frac{L_1}{K_1} + \frac{L_2}{K_2} \right] \tag{26}$$

where A_{w} is the area of front and back wall surface.

In a similar way, the side and bottom wall conductive heat losses can be determined

$$Q_{\mathrm{sw}} = \frac{T_{\mathrm{swi}} - T_{\mathrm{swo}}}{R_{\mathrm{sw}}} \tag{27}$$

$$Q_{\mathrm{bot}} = \frac{T_{\mathrm{b}} - T_{\mathrm{bot}}}{R_{\mathrm{bot}}} \tag{28}$$

Apart from above-mentioned losses, there is a possibility of heat loss due to leakages in the joints, fittings, etc. which is termed as unaccountable heat loss and determined using the following equation

$$Q_{\text{un}} = I - [Q_{\text{d}} + Q_{\text{rg}} + Q_{\text{cg}} + Q_{\text{bw}} + Q_{\text{sw}} + Q_{\text{bot}} + Q_{\text{sww}}] \tag{29}$$

where I is the solar intensity falling on the surface, W/m^2.

The overall efficiency of the solar still is

$$\eta_o = \frac{Q_{\text{d}}}{I} \tag{30}$$

3 Case Study

This case study explores the applicability of theoretical modeling of simple solar still for the prediction of performance of the system and also compared with the experimental results to test the accuracy. Moreover, the effect of various parameters such as water depth, sponge liner thickness, sponge liner color, and energy storage materials are also discussed.

For this case study, the experimental results of Arjunan et al. [44, 51–53] were considered. They have developed two identical single slope simple stills for conducting the experimental studies for analyzing the effect of various parameters. The schematic and pictorial views of the developed experimental setup are shown in Figs. 9 and 10, respectively. The experimental setups were fabricated with the effective basin area of 1000 mm × 500 mm using 1.4-mm-thick galvanized iron sheets. The lower and higher vertical side heights of the basin were of 200 and 280 mm, respectively. The top of the still was covered with a 4-mm-thick glass to condensate the vapor from the basin. All the sidewalls and bottom sides were insulated to avoid heat loss to the surroundings and also the glass cover was fixed on the top with a wooden frame along with the gaskets to facilitate the better operation through the reduction of leakages. The specifications of the experimental setup are given in Table 1.

In order to evaluate the productivity of the still, the temperature values of the basic components of the simple still are to be determined by solving the nonlinear equations arrived from the energy balance equations with the help of any computational solution methods. The input parameters considered for the theoretical model are given in Table 2.

The experimental results of simple solar still were reported for the effect of various parameters such as water depth, sponge liner thickness, sponge liner color, and energy storage materials. The following section compares the experimental results with the theoretical results predicted using the theoretical model.

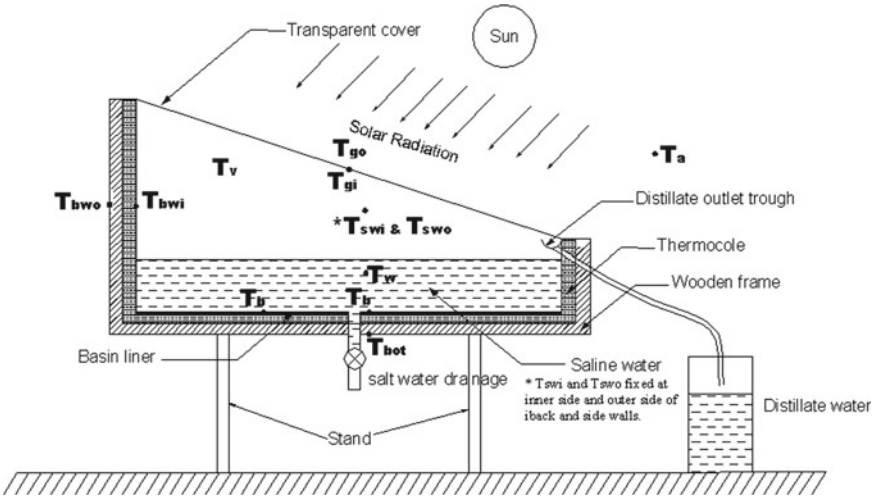

Fig. 9 Schematic diagram of experimental setup

Fig. 10 Pictorial view of experimental setup [44]

3.1 Effect of Water Depth in the Basin

The effect of water depth in the basin of the still is considered as one of the important parameters, so they have carried out the experimental studies for different water depths from 10 to 60 mm in the basin. Based on the experimental study, they reported that the maximum productivity of the still was 1.72 kg/day was attained at the depth of 20 mm. The theoretical value for the typical water depth of 20 mm was determined using the mathematical model, and the results were compared with the experimental values. Figures 11 and 12 illustrate the comparison of the experimental and theoretical values. It is observed that the theoretical results are having good agreement with the experimental values.

Table 1 Specification of the experimental setup [44]

Specification	Values
Basin area (A_b)	0.5 m^2
Glass area (A_g)	0.508 m^2
Back wall surface area (A_{bw})	0.488 m^2
Sidewall surface area (A_{sw})	0.234 m^2
Latent heat of vaporization for water (h_{fg})	2382.9 kJ/kg
Glass emissivity (ε_g)	0.88
Water emissivity (ε_w)	0.96
Air-vapor mixture depth (d_f)	0.144 m
Thickness of insulation layer 1 (thermocol)	25.4 mm
Thermal conductivity of layer 1	0.015 W/mK
Thickness of insulation layer 2 (wood)	12.5 mm
Thermal conductivity of layer 2	0.055 W/mK

Table 2 Design parameters of solar still for theoretical simulation

Notations	Dimensions
A	0.5 m^2
m	10 kg
α_g	0.0475
α_b	0.96
h_{cg}	8.8 W/m^2
h_{rg}	7.3 W/m^2
C_{pw}	4186 J/kg K
α_w	0.05
h_{ew}	28.5 W/m^2 K
h_a	1.29 W/m^2/K
U_{bot}	7.0 W/m^2 K
T_a	30 °C

3.2 Effect of Sponge Liner Thicknesses

In simple solar still, the solar radiation falling on the basin inner walls is partially reflected to the other basin components such as glass cover, basin water, vapor, and the remaining part of energy is stored by the walls, which is usually lost to the environment through convection. The maximum available energy at the basin walls can be utilized by covering the entire inner wall surfaces using sponge liners. Introducing the sponge liner in the basin walls, increases the productivity of the still through the following ways; (i) by raising the basin saline water through the sponge liner cavities due to capillary effect, (ii) absorbing the maximum radiation falling on the inner wall surface, and (iii) reducing the temperature difference between the glass

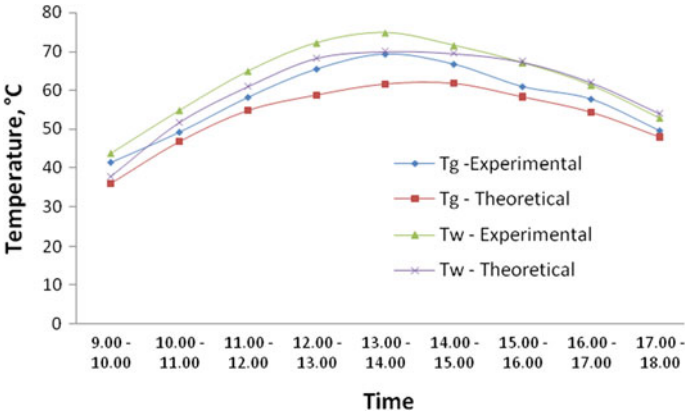

Fig. 11 Theoretical versus experimental temperatures of water and glass for 20 mm water depth

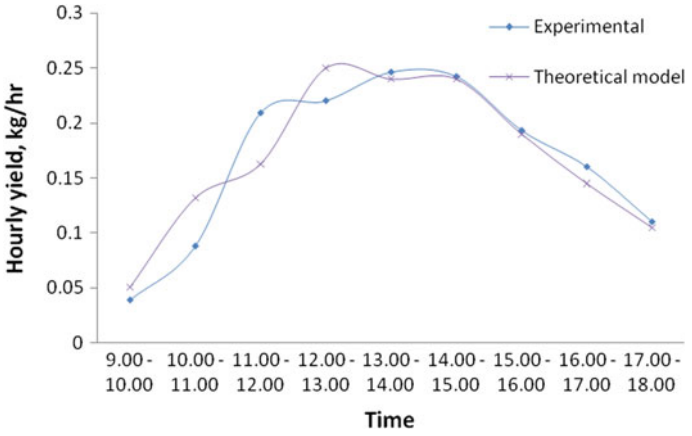

Fig. 12 Theoretical versus experimental output for 20 mm water depth

cover and the basin water by absorbing a portion of vapour inside the still. And also sponge liner reduces the heat loss from inner wall surfaces to the other components, which results in a reduction of operating temperatures of the still components when compared with conventional simple still. Moreover, the sponge liner materials are easily available at low cost.

The experimental study results for the effect of sponge liner reported by Arjunan et al. [51] are compared with the theoretical results. The productivity of the solar still was increased by increasing the temperature difference between basin water and glass cover through the use of sponge liners inside the basin walls. The pictorial view of the sponge liner arrangement is shown in Fig. 13. They have conducted the studies with different liner thicknesses such as 3, 5, 7, 10, and 12 mm, and the water depth was maintained at 20 mm for all experimental studies. The determined the

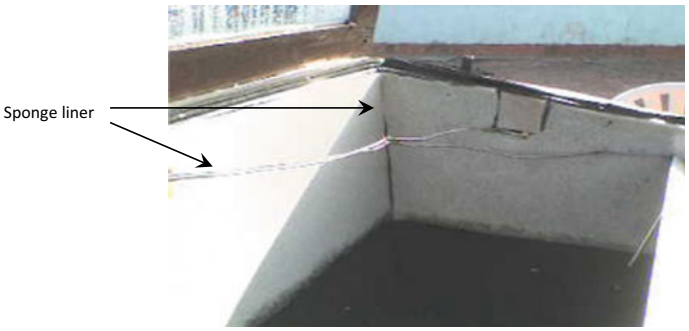

Fig. 13 Photographic image of sponge liner surfaces [51]

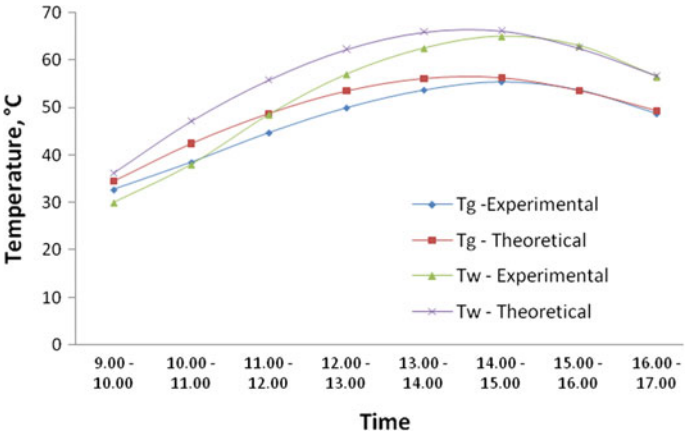

Fig. 14 Theoretical versus experimental temperatures of water and glass for 5-mm-thick sponge liner

optimum thickness of the sponge liner. The maximum output per day (1.54 kg/day) was observed at 5-mm-thick sponge liner. The experimental and theoretical temperature values of basin water and glass cover are compared in Fig. 14 for 5-mm-thick sponge liner, and it clearly indicates that the predicted values are matching with the experimental results. The theoretical output of the still is also compared with the experimental output for 5-mm-thick sponge liner as shown in Fig. 15. Hence, the remaining experimental studies such as the effect of sponge liner color and combined effect of sponge liner and energy storage materials have been conducted with 5-mm-thick sponge liner.

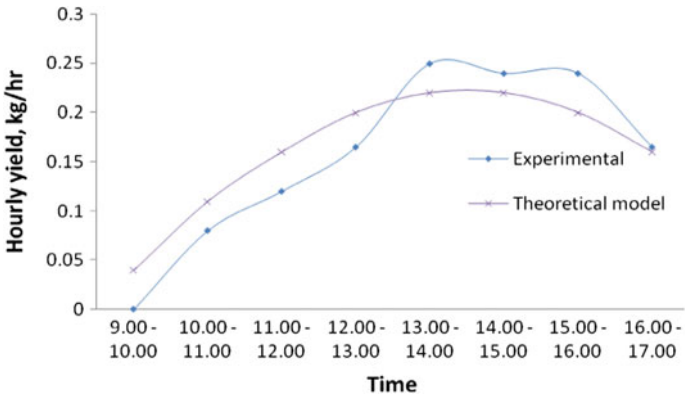

Fig. 15 Theoretical versus experimental output for 5-mm-thick sponge liner

3.3 Effect of Sponge Liner Color

The sponge liner inside the basin wall increases the productivity of the still and the color of the sponge liner also affects the output of the still. The experimental study was conducted using basic colors such as blue, black, green, white, and red. Based on the previous results as discussed in Sect. 3.2, the 5-mm-thick sponge liner is found to provide higher yield. Therefore, in this experimental study, the sponge liner thickness is considered as 5 mm. It is observed from the experimental observation that the black colored sponge liner provides an output yield higher than the other colored sponge liners. Hence, the black colored sponge liner has been selected for use in the combined energy storage medium still. The experimental and theoretical temperatures of basin water and glass cover are compared for black colored sponge liner is in Fig. 16.

3.4 Effect of Energy Storage Medium

The solar radiation is usually higher during the noon periods, which leads to higher temperature of glass cover and water in basin. The higher glass cover temperature results in poor condensation rate of air-water vapor mixture at exposed glass surface. For an efficient solar desalination system, it is necessary to have an improved production rate. Many researchers have attempted to enhance the production rate of the conventional solar still through the modifications such as increasing temperature of the basin water, decreasing the temperature of glass cover, maximizing the utilization of available energy through the reduction of heat losses and storing it for later use. Among these methods, usage of energy storage materials in the basin is identified as an easy and less expensive method of maximizing the available energy. The simple

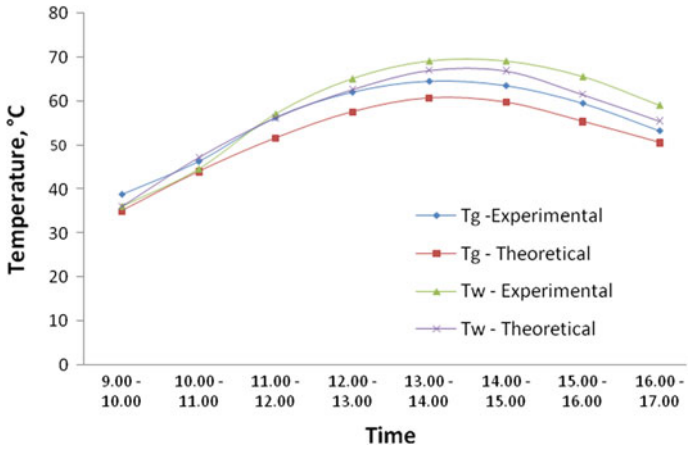

Fig. 16 Theoretical versus experimental temperatures of water and glass for black colored sponge liner

Table 3 Properties of energy storage materials

S. No.	Energy storage material	Size (mm)	Quantity (kg)	Specific heat capacity (kJ/kg K)
1	Blue metal stone	10–15	5	770
2	Black granite gravels	10–15	5	740
3	Pebbles	10–15	5	840
4	Paraffin wax	–	2	2140

method of incorporating the energy storage materials inside the conventional solar still is shown in Fig. 18.

In the case study considered, the authors have used different energy storage materials to store the excessive energy available in the water basin. The materials used were of blue metal stones, granites, pebbles, and paraffin wax. Eight numbers of 12-mm-diameter tubes were used to fill paraffin wax, and the tubes were placed inside the water basin. These materials were selected for the study as they are easily available at low cost. The properties of the materials are listed in Table 3.

The purpose of this study is to find the effect of energy storage materials on the performance of the simple solar still, and the materials selected were having lower heat capacity when compared with the saline water.

It is also included to find the efficient low-cost energy storage material for typical solar still among black granite gravel, pebbles, blue metal stones, and paraffin wax. The higher yield in the solar still was observed when the black granite gravels are used as energy storage medium (Table 4). It is understood that black granite gravels are efficient than other energy storage materials which are used for this experimental study. Hence, black granite gravels are used as energy storage material in the combination of black sponge liner still which is discussed in the next section.

Table 4 Comparative performance study of simple solar still with different parameters

S. No.	Parameters	Distilled output (kg)	Highest output (kg)	Average improvement from the conventional still (%)
Effect of water depth (mm)				
1	10	1.64	1.72 (20 mm water depth)	17.0
2	20	1.72		
3	30	1.59		
4	40	1.56		
5	50	1.49		
6	60	1.47		
Effect of sponge liner thickness (mm)				
1	No sponge (conventional)	1.14	1.54 (5-mm thick sponge liner)	35.2
2	3	1.31		
3	5	1.54		
4	7	1.33		
5	10	1.32		
6	12	1.21		
Effect of sponge liner color				
1	Green	1.55	1.63 (Black colored sponge liner)	43.4
2	Red	1.47		
3	Blue	1.45		
4	Black	1.63		
5	White	1.54		
Effect of energy storage materials				
1	Pebbles	1.17	1.29 (black granite gravels)	10.3
2	Blue metal stones	1.19		
3	Black granite gravels	1.29		
4	Paraffin wax	1.27		
Combined effect of sponge liner and energy storage materials				
1	Black granite gravels and black sponge liner	1.71	1.71	50.6

3.5 *Combined Effect of Sponge Liner and Energy Storage Materials*

Based on higher yield, from the previous experimental studies, the following parameters are used for this study:

(i) Water depth is 20 mm
(ii) Thickness of sponge liner is 5 mm
(iii) Black colored sponge liner
(iv) The black granite gravel

The schematic arrangement of this combination is given in Fig. 22.

This experimental study is carried with the combined effect of all the parameters which are mentioned above. It is observed that the output is increased by more than 50% when the combination of the above-said parameters is used in the still, which is evident in Table 4.

By comparing Figs. 11, 12, 13, 14, 15, 16, 17, 18, 19, 20, 21, 22, 23, and 24, it is noted that the theoretical values are having good agreement with the experimental values for all the cases, and the deviations are in the acceptable range. The theoretical value of hourly output is higher during the morning hours when compared with the experimental value, due to the heat absorption of still components. During the noon and afternoon hours, the values of theoretical and experimental hourly yield are very closely matching. In the evening hours, the hourly yields of experimental values are higher than the theoretical values. The fact behind the increase in the yield is due to the reason that the release of excessive energy stored by the components of the still. The productivity of simple solar still for per day is calculated for all the cases using the theoretical models and they are compared in Table 5. The table indicates that the theoretical models are capable of predicting the performance of the system with negligible error percentage, i.e., less than 5% from the experimental results presented in case study section. The deviation of theoretical results from the experimental results may be due the following reasons: (i) the absorption and reflection coefficients of glass cover and basin water are assumed as constant, but in practical it varies with respect to time and temperature, (ii) the alteration in transmission coefficients of glass cover is accounted in theoretical model, (iii) the heat transfer coefficients are assumed as constant but they are varying with respect to temperature.

A typical cumulative energy balance for different water depth analyses is given in Table 6. The table clearly indicates the amount of heat transfer lost/utilized during the conversion process, and further information will be very useful to understand the system operation very well. The maximum amount of heat lost to the atmosphere is through convection as well as radiation from the glass cover of the system for all water depths. The conductive heat losses from side and bottom wall surfaces are considerably low. Apart from all energy transfer, unaccountable losses are noticed in the energy balance of the system, which may be due to the vapor leakage through gaskets, joints, and sensible heat stored by the still elements such as glass cover, water, basin liner, absorber plate, etc. The unaccounted losses are found quite high in

Table 5 Theoretical versus experimental output for different parameters

S. No.	Parameters	Distilled output (kg)		Deviation (%)
		Exp	Theo	
Effect of water depth (mm)				
1	10	1.64	1.72	4.8
2	20	1.72	1.80	4.6
3	30	1.59	1.56	1.9
4	40	1.56	1.58	1.3
5	50	1.49	1.51	1.5
6	60	1.47	1.53	4.0
Average deviation (%)				3.0
Effect of sponge liner thickness (mm)				
1	No sponge	1.14	1.18	3.5
2	3	1.31	1.43	9.2
3	5	1.54	1.52	1.4
4	7	1.33	1.38	3.7
5	10	1.32	1.36	3.0
6	12	1.21	1.30	7.4
Average deviation (%)				4.1
Effect of sponge liner color				
1	White	1.54	1.52	1.4
2	Red	1.47	1.48	0.68
3	Green	1.55	1.60	3.2
4	Black	1.63	1.78	9.2
5	Blue	1.45	1.49	2.8
Average deviation (%)				3.5
Effect of energy storage materials				
1	Pebbles	1.17	1.21	3.4
2	Blue metal stones	1.19	1.24	4.2
3	Black granite gravels	1.29	1.25	3.1
4	Paraffin wax	1.27	1.35	4.7
Combination of sponge liner and energy storage materials				
1	Black granite gravels and black sponge liner	1.71	1.72	0.60
Average deviation (%)				3.1
Overall deviation (%)				3.68

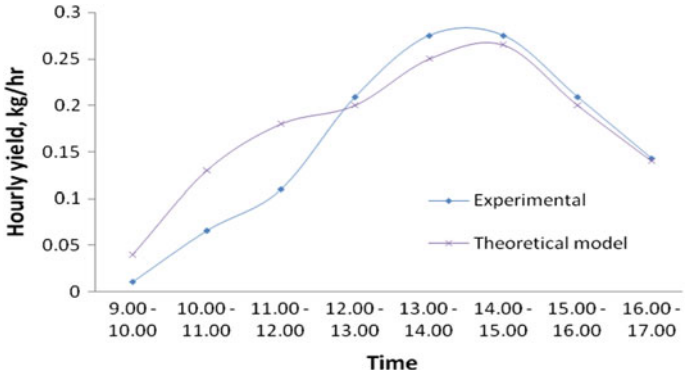

Fig. 17 Theoretical versus experimental output for black colored sponge liner

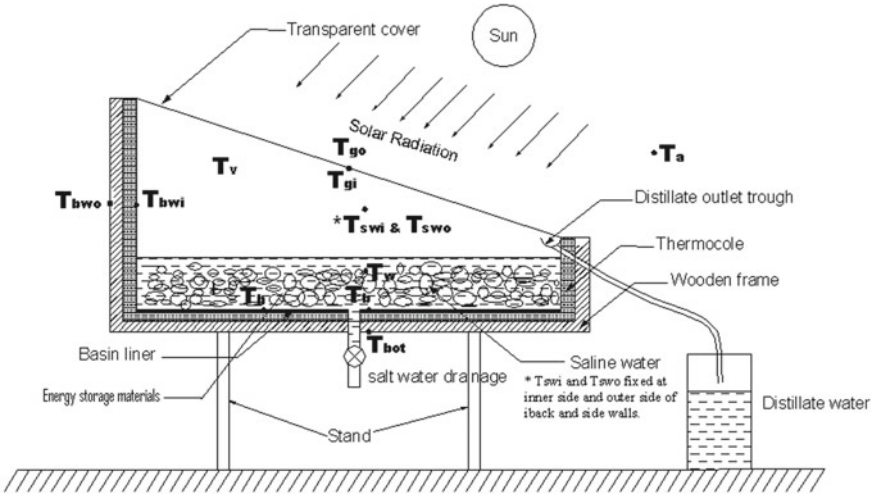

Fig. 18 Schematic arrangement of energy storage material in the simple solar still [52]

the higher water depths at 40, 50, and 60 mm, due to the higher heat storage capacity. The cumulative heat balances for the other experimental studies such as effect of sponge liner and effect of colored sponge liner are found to be closely matched with the 20-mm water depth study.

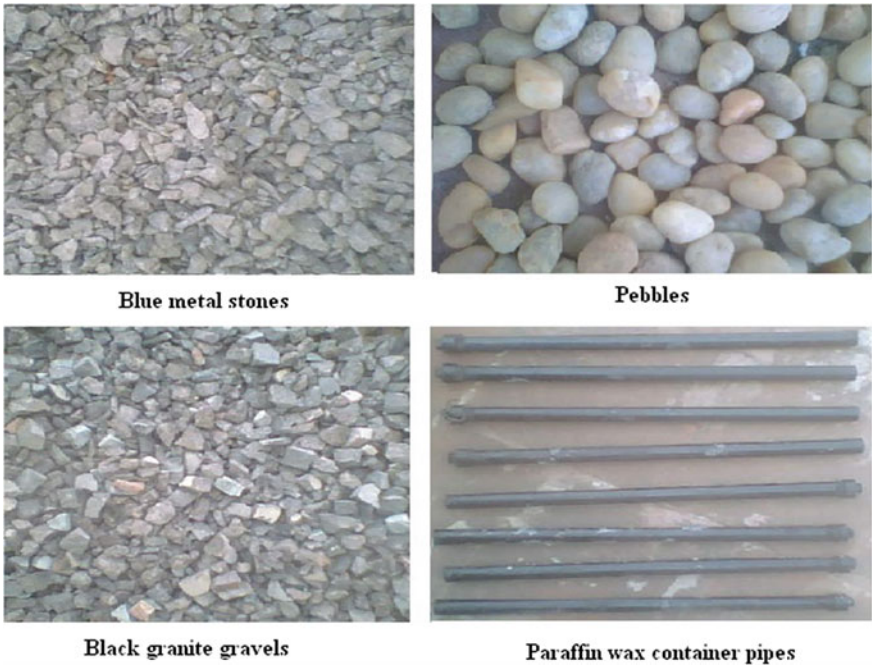

Fig. 19 Different energy storage materials [52]

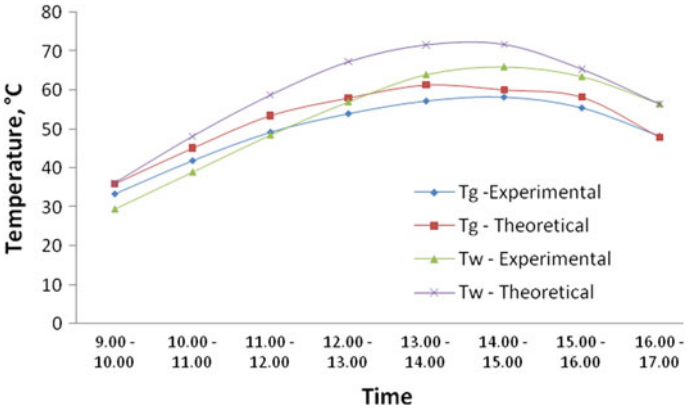

Fig. 20 Theoretical versus experimental temperatures of water and glass for black granite gravels

Table 6 Heat balance of still for different water depths

S. No.	Description		Amount of heat transfer, W					
			10 mm	20 mm	30 mm	40 mm	50 mm	60 mm
1	Radiation loss Glass cover to atmosphere	Q_{rg}	820.63	801.77	693.98	625.13	597.62	577.10
2	Convection loss glass Cover to atmosphere	Q_{cg}	535.10	545.16	473.69	412.22	380.62	364.92
3	Conduction loss Inside wall to outside wall through	Q_{bw}	44.64	43.79	35.49	36.95	38.4	65.21
4	Conduction loss Inside to atmosphere through sidewalls	Q_{sw}	20.22	23.7	21.25	14.31	19.8	18.29
5	Conduction loss Inside to outer side through bottom	Q_{bot}	29.94	31.9	27.52	22.71	22.63	19.46
6	Conduction loss Basin water vertical surface to atmosphere	Q_{sww}	2.34	2.59	2.37	1.41	1.74	1.18
7	Amount of heat utilized for the conversion of saline to pure water	Q_d	1083.56	1136.51	1052.45	1045.83	982.95	972.36
8	Un accountable heat loss (due to vapor leakage, heat loss through joints, etc.)	Q_u	223.56	166.68	434.50	656.52	685.86	761.48

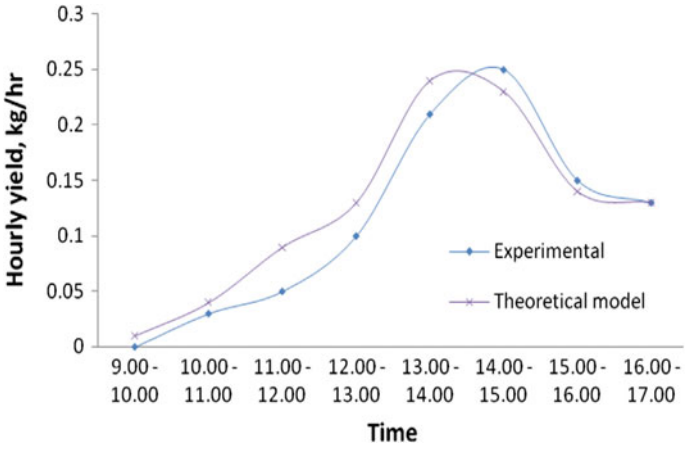

Fig. 21 Theoretical versus experimental output for black granite gravels

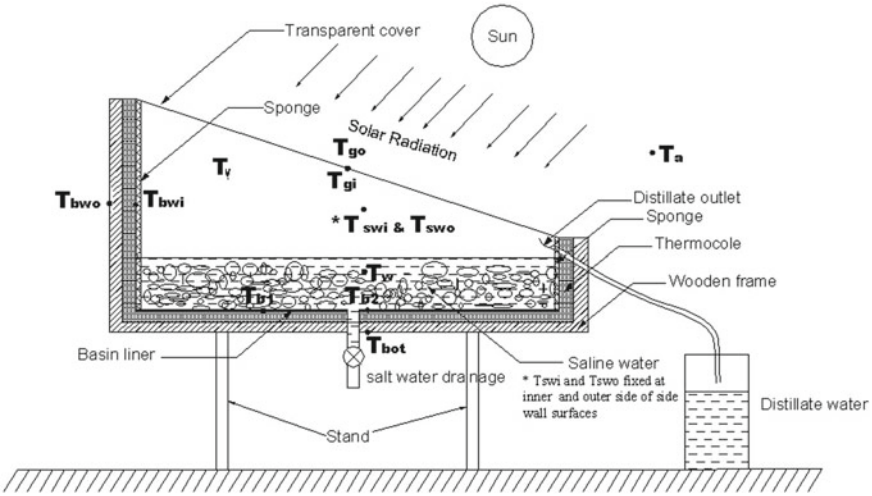

Fig. 22 Schematic arrangements of sponge liner and energy storage material

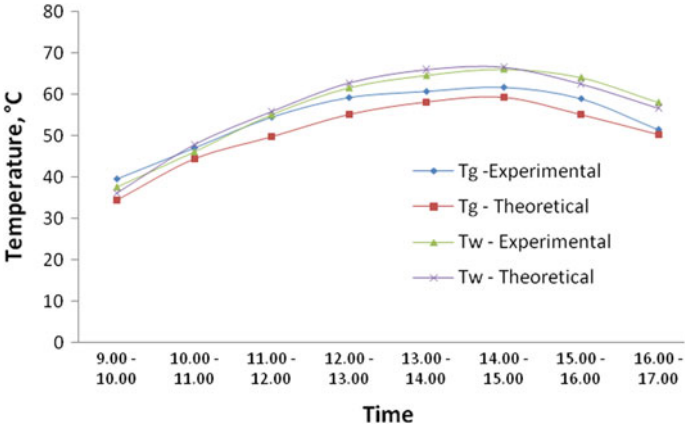

Fig. 23 Theoretical versus experimental temperatures of water and glass for the combination of black granite gravels and black sponge liner

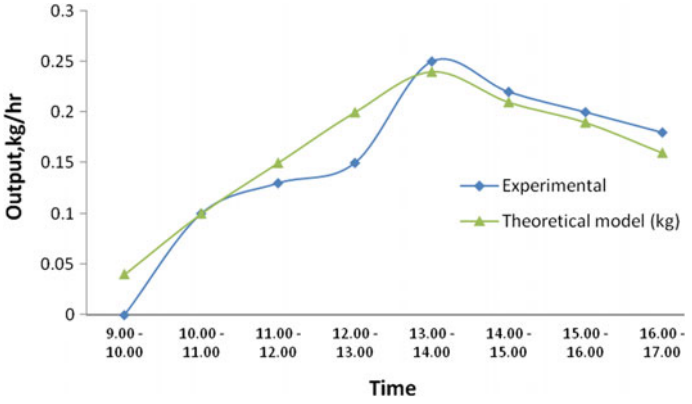

Fig. 24 Theoretical versus experimental output for the combination of black granite gravels and black sponge liner

4 Conclusions

This chapter presents an overview of theoretical modeling procedure for simple solar desalination system and also reports the significant design and operational parameters of the system which affect the performance are tilt angle, thickness of glass, additional condensers, reflectors, phase-change materials, flat plate and ETC collectors, nanofluids, basin water temperature, water depth, etc. An efficient solar desalination system can be designed with thorough knowledge on the performance and the effect of various parameters. Developing theoretical model for solar desalination systems is an attractive alternative solution to develop and investigate enhanced designs under different operational and climatically conditions. The theoretical models are very simple and effective tools to design the system with various performance enhancement methods such as usage of energy storage materials and sponge liners. This chapter also explores the capability of the theoretical models along with the case study.

References

1. Rajvanshi AK (1981) Effect of various dyes on solar distillation. Sol Energy 27(1):51–65
2. Okeke CE, Egarievwe SU, Animalu AOE (1990) Effects of coal and charcoal on solar-still performance. Energy 15(11):1071–1073
3. Ouar MA, Sellami MH, Meddour SE, Touahir R, Guemari S, Loudiyi K (2017) Experimental yield analysis of groundwater solar desalination system using absorbent materials. Groundw Sustain Dev 5:261–267
4. Kabeel AE, Abdelgaied M, Eisa A (2018) Enhancing the performance of single basin solar still using high thermal conductivity sensible storage materials. J Clean Prod 183:20–25
5. Deshmukh HS, Thombre SB (2017) Solar distillation with single basin solar still using sensible heat storage materials. Desalination 410:91–98
6. Faegh M, Shafii MB (2017) Experimental investigation of a solar still equipped with an external heat storage system using phase change materials and heat pipes. Desalination 409:128–135
7. Sharshir SW, Peng G, Wu L, Essa FA, Kabeel AE, Yang N (2017) The effects of flake graphite nanoparticles, phase change material, and film cooling on the solar still performance. Appl Energy 191:358–366
8. Panchal H, Patel DK, Patel P (2018) Theoretical and experimental performance analysis of sandstones and marble pieces as thermal energy storage materials inside solar stills. Int J Ambient Energy 39(3):221–229
9. Arjunan TV, Aybar HŞ, Nedunchezhian N (2017) Experimental study on enhancing the productivity of solar still using locally available material as a storage medium. J Inst Eng (India) Ser C 98(2):191–196
10. Panchal H, Patel P, Patel N, Thakkar H (2017) Performance analysis of solar still with different energy-absorbing materials. Int J Ambient Energy 38(3):224–228
11. Sarhaddi F, Tabrizi FF, Zoori HA, Mousavi SAHS (2017) Comparative study of two weir type cascade solar stills with and without PCM storage using energy and exergy analysis. Energy Convers Manag 133:97–109
12. Kaushal AK, Mittal MK, Gangacharyulu D (2017) An experimental study of floating wick basin type vertical multiple effect diffusion solar still with waste heat recovery. Desalination 414:35–45

13. Sharon H, Reddy KS, Krithika D, Philip L (2017) Experimental performance investigation of tilted solar still with basin and wick for distillate quality and enviro-economic aspects. Desalination 410:30–54
14. Pal P, Yadav P, Dev R, Singh D (2017) Performance analysis of modified basin type double slope multi–wick solar still. Desalination 422:68–82
15. Kabeel AE, Teamah MA, Abdelgaied M, Aziz GBA (2017) Modified pyramid solar still with v-corrugated absorber plate and PCM as a thermal storage medium. J Clean Prod 161:881–887
16. Rufuss DDW, Iniyan S, Suganthi L, Davies PA (2017) Nanoparticles enhanced phase change material (NPCM) as heat storage in solar still application for productivity enhancement. Energy Procedia 141:45–49
17. Arunkumar T, Kabeel AE (2017) Effect of phase change material on concentric circular tubular solar still-integration meets enhancement. Desalination 414:46–50
18. Kabeel AE, El-Samadony YAF, El-Maghlany WM (2017) Theoretical performance comparison of solar still using different PCM. In: Twentieth international water technology conference, IWTC20, pp 424–432
19. Shanmugan S, Palani S, Janarthanan B (2018) Productivity enhancement of solar still by PCM and nanoparticles miscellaneous basin absorbing materials. Desalination 433:186–198
20. Al-harahsheh M, Abu-Arabi M, Mousa H, Alzghoul Z (2018) Solar desalination using solar still enhanced by external solar collector and PCM. Appl Therm Eng 128:1030–1040
21. Mahian O, Kianifar A, Heris SZ, Wen D, Sahin AZ, Wongwises S (2017) Nanofluids effects on the evaporation rate in a solar still equipped with a heat exchanger. Nano Energy 36:134–155
22. Rashidi S, Akar S, Bovand M, Ellahi R (2018) Volume of fluid model to simulate the nanofluid flow and entropy generation in a single slope solar still. Renew Energy 115:400–410
23. Thakur AK, Agarwal D, Khandelwal P, Dev S (2018) Comparative study and yield productivity of nano-paint and nano-fluid used in a passive-type single basin solar still. In: Advances in smart grid and renewable energy. Springer, Singapore, pp 709–716
24. Kabeel AE, Omara ZM, Essa FA (2017) Numerical investigation of modified solar still using nanofluids and external condenser. J Taiwan Inst Chem Eng 75:77–86
25. Rashidi S, Bovand M, Rahbar N, Esfahani JA (2018) Steps optimization and productivity enhancement in a nanofluid cascade solar still. Renew Energy 118:536–545
26. Chen W, Zou C, Li X, Li L (2017) Experimental investigation of SiC nanofluids for solar distillation system: stability, optical properties and thermal conductivity with saline water-based fluid. Int J Heat Mass Transf 107:264–270
27. Sharshir SW, Peng G, Wu L, Yang N, Essa FA, Elsheikh AH, Kabeel AE (2017) Enhancing the solar still performance using nanofluids and glass cover cooling: experimental study. Appl Therm Eng 113:684–693
28. Kerfah R, Noura B, Meraimi Z, Zeghmati B (2017) Experimental investigation of basin solar still with additional condensation chamber under Algerian climatic conditions. J Renew Sustain Energy 9(3):033704
29. Suganthi L, Iniyan S, Rufuss DDW (2018) Combined effect of heat storage, reflective material, and additional heat source on the productivity of a solar still—techno-economic approach. J Test Eval 46(6)
30. Panchal HN, Shah PK (2013) Performance analysis of double basin solar still with evacuated tubes. Appl Solar Energy 49(3):174–179
31. Dhindsa GS, Mittal MK (2018) Experimental study of basin type vertical multiple effect diffusion solar still integrated with mini solar pond to generate nocturnal distillate. Energy Convers Manag 165:669–680
32. Panchal H, Mohan I (2017) Various methods applied to solar still for enhancement of distillate output. Desalination 415:76–89
33. Rahimi-Ahar Z, Hatamipour MS, Ghalavand Y (2018) Experimental investigation of a solar vacuum humidification-dehumidification (VHDH) desalination system. Desalination 437:73–80
34. El-Samadony YAF, Kabeel AE (2014) Theoretical estimation of the optimum glass cover water film cooling parameters combinations of a stepped solar still. Energy 68:744–750

35. Mousa HA (1997) Water film cooling over the glass cover of a solar still including evaporation effects. Energy 22(1):43–48
36. Mazraeh AE, Babayan M, Yari M, Sefidan AM, Saha SC (2018) Theoretical study on the performance of a solar still system integrated with PCM-PV module for sustainable water and power generation. Desalination 443:184–197
37. Dumka P, Mishra DR (2018) Energy and exergy analysis of conventional and modified solar still integrated with sand bed earth: Study of heat and mass transfer. Desalination 437:15–25
38. Muftah AF, Sopian K, Alghoul MA (2018) Performance of basin type stepped solar still enhanced with superior design concepts. Desalination 435:198–209
39. Xie G, Sun L, Yan T, Tang J, Bao J, Du M (2018) Model development and experimental verification for tubular solar still operating under vacuum condition. Energy 157:115–130
40. Naroei M, Sarhaddi F, Sobhnamayan F (2018) Efficiency of a photovoltaic thermal stepped solar still: experimental and numerical analysis. Desalination 441:87–95
41. Rahbar N, Asadi A, Fotouhi-Bafghi E (2018) Performance evaluation of two solar stills of different geometries: tubular versus triangular: experimental study, numerical simulation, and second law analysis. Desalination 443:44–55
42. Kalbasi R, Alemrajabi AA, Afrand M (2018) Thermal modeling and analysis of single and double effect solar stills: an experimental validation. Appl Therm Eng 129:1455–1465
43. Malaeb L, Aboughali K, Ayoub GM (2016) Modeling of a modified solar still system with enhanced productivity. Sol Energy 125:360–372
44. Arjunan TV, Aybar HŞ, Nedunchezhian N (2011) Effect of sponge liner on the internal heat transfer coefficients in a simple solar still. Desalin Water Treat 29(1–3):271–284
45. Badran OO, Abu-Khader MM (2007) Evaluating thermal performance of a single slope solar still. Heat Mass Transf 43(10):985–995
46. Edalatpour M, Kianifar A, Ghiami S (2015) Effect of blade installation on heat transfer and fluid flow within a single slope solar still. Int Commun Heat Mass Transfer 66:63–70
47. Chen Z, Yao Y, Zheng Z, Zheng H, Yang Y, Hou LA, Chen G (2013) Analysis of the characteristics of heat and mass transfer of a three-effect tubular solar still and experimental research. Desalination 330:42–48
48. Singh AK, Tiwari GN (1993) Thermal evaluation of regenerative active solar distillation under thermosyphon mode. Energy Convers Manag 34:697–706
49. El-Samadony YAF, El-Maghlany WM, Kabeel AE (2016) Influence of glass cover inclination angle on radiation heat transfer rate within stepped solar still. Desalination 384:68–77
50. Prakash J, Kavathekar AK (1986) Performance prediction of a regenerative solar still. Solar & Wind Technology 3(2):119–125
51. Arjunan TV, Aybar HŞ, Nedunchezhian N (2011) The effect of sponge liner on the performance of simple solar still. Int J Renew Energy Technol 2(2):169–192
52. Arjunan TV, Aybar H, Neelakrishnan S, Sampathkumar K, Amjad S, Subramanian R, Nedunchezhian N (2012) The effect of sponge liner colors on the performance of simple solar stills. Energy Sour Part A Recovery Util Environ Effects 34(21):1984–1994
53. Arjunan TV, Aybar HS, Sadagopan P, SaratChandran B, Neelakrishnan S, Nedunchezhian N (2014) The effect of energy storage materials on the performance of a simple solar still. Energy Sources Part A Recovery Util Environ Effects 36(2):131–141